CLINICAL AND VACCINE IMMUNOLOGY, Apr. 2007, p. 412–419 Vol. 14, No. 4
1556-6811/07/$08.00+0 doi:10.1128/CVI.00372-06

An Immunomagnetic Single-Platform Image Cytometer for Cell Enumeration Based on Antibody Specificity▽

Xiao Li,[1]* Arjan G. J. Tibbe,[2] Erik Droog,[1] Leon W. M. M. Terstappen,[3] and Jan Greve[1]

Biophysical Engineering Group, Faculty of Science and Technology, University of Twente, Dienstweg 1, Building Zuidhorst, 7522 ND Enschede,[1] and Immunicon Europe Inc., Hengelosestraat 705, 7521 PA Enschede,[2] The Netherlands, and Immunicon Inc., 3401 Masons Mill Rd., Huntingdon Valley, Pennsylvania 19006[3]

Received 8 October 2006/Returned for modification 11 December 2006/Accepted 27 January 2007

Simplification of cell enumeration technologies is necessary, especially for resource-poor countries, where reliable and affordable enumeration systems are greatly needed. In this paper, an immunomagnetic single-platform image cytometer (SP ICM) for cell enumeration based on antibody specificity is reported. A chamber/magnet assembly was designed such that the immunomagnetically labeled, acridine orange-stained cells in a blood sample moved to the surface of the chamber, where a fluorescent image was captured and analyzed for cell enumeration. The system was evaluated by applying one kind of antibody to count leukocytes and one kind for each leukocyte subpopulation: CD45 for leukocytes, CD3 for T lymphocytes, and CD19 for B lymphocytes. Excellent precision and linearity were achieved. Moreover, these cell counts, each from blood specimens of 42 to 52 randomly selected patients, were compared with those obtained by SP (TruCount) and dual-platform (DP) flow cytometry (FCM) technologies. The cell counts obtained by our system were in between those obtained from the TruCount and DP FCM methods; and good correlations were achieved ($R \geq 0.95$). For $CD4^+$ counts, as we expected, the cell count by our system was significantly higher than the $CD4^+$ T-lymphocyte counts obtained by SP and DP FCM methods. Immunophenotyping of the immunomagnetically selected $CD4^+$ cells showed that, besides $CD4^+$ T lymphocytes, a proportion of the $CD4^+$ dim monocytes was also selected. Our system is a simple immunomagnetic SP ICM, which can potentially be used for enumeration of $CD3^+$ $CD4^+$ T lymphocytes in resource-poor countries if an additional CD3 immunofluorescent label is applied.

Absolute enumeration of cells in clinical samples is becoming more and more important. Examples include enumeration of leukocytes and leukocyte subpopulations in the blood of patients, enumeration of residual leukocytes in leukocyte-depleted blood transfusion products (4), and enumeration of circulating tumor cells in the peripheral blood of cancer patients (13, 18).

Absolute cell enumeration is usually accomplished by single-platform (SP) and dual-platform (DP) flow cytometry (FCM) methods. SP FCM methods use calibration beads (20) or employ a volumetric method (8). DP FCM technologies calculate the absolute number of cells of one or more subpopulations by multiplying the absolute cell count obtained by an automatic hematology analyzer by the percentage of each specific cell subpopulation obtained by FCM (6). The DP FCM methods are usually less accurate than the SP FCM methods because of differences among hematology analyzers (19). In general, both SP and DP methods are expensive with regard to equipment, maintenance, and technician training (14). Consequently, it is important to develop simpler SP cell enumeration technologies.

We developed an immunomagnetic method using an SP image cytometer (ICM) to enumerate leukocytes and leukocyte subpopulations that can be uniquely characterized by one specific type of antibody. This method is realized by using "cellular astronomy" technology (21), e.g., light-emitting diodes (LEDs) for illumination and a smart camera for imaging and analyzing the images obtained. In our method, the target cells are immunomagnetically labeled and fluorescently stained with acridine orange (AO). The labeled cells from a known volume of sample are then driven by a magnetic force to a surface of an analysis chamber, where these cells are illuminated using LEDs (22). A fluorescent image of the target cells at the surface is captured by a smart charge-coupled device (CCD) camera with software that counts the cells and calculates the number of cells per microliter of whole blood. The method yields absolute cell counts. The system is easy to handle and is battery operated.

In this paper, we demonstrate the performance of our cell enumeration system in counting $CD45^+$ leukocytes, $CD3^+$ T lymphocytes, and $CD19^+$ B lymphocytes in human whole blood. The immunomagnetic selections of these cells are governed by their antibody specificities. By comparing the cell counts obtained from our SP ICM method to those from the SP and DP FCM methods, the accuracy of our system is assessed. In cases where the immunomagnetic label used is not specific for only one type of cell subpopulation, as for $CD4^+$ cells, both $CD4^+$ T lymphocytes and $CD4^{dim}$ monocytes (7) are selected. Additional immunolabeling should be applied to accurately enumerate $CD4^+$ T lymphocytes for human immunodeficiency virus (HIV) staging. In a forthcoming paper, we will deal with this challenge.

* Corresponding author. Mailing address: Faculty of Science and Technology, Biophysical Engineering Group, University of Twente, Dienstweg 1, Building Zuidhorst, 7522 ND Enschede, The Netherlands. Phone: 31 53 4893870. Fax: 31 53 4891105. E-mail: l.x.lixiao@tnw.utwente.nl.

▽ Published ahead of print on 7 February 2007.

MATERIALS AND METHODS

ICM instrumentation. The instrument is in principle a simple SP ICM based on an automated fluorescence microscope (Fig. 1). The optical components consist of two 5-mW LEDs (Marl 110106; Nichia, Japan), a 10× objective (LOMO Optics, Germantown, MD), and an emission filter (RG 540; Schott, Germany). Images are captured and processed with a smart CCD camera (1,300 × 1,030 pixels; VC67; Vision Components, Germany). Upon insertion of an analysis chamber into the instrument, a microswitch starts the measuring cycle. The camera software then controls all further steps, and the captured images are analyzed using a homemade image analysis program. The number of cells per microliter of whole blood is displayed on a liquid crystal display (LCD). The system operates on a 12-V rechargeable battery, which can last for about 400 tests. The overall dimensions of the cell enumeration system are 17 cm by 17 cm by 19 cm (Fig. 1A).

Cell enumerations with the SP ICM. (i) Blood collection. Blood specimens were collected in sterile K_3 EDTA Vacutainer blood collection tubes (BD Biosciences). Blood specimens from randomly selected HIV-negative patients were supplied by the local hospital (Medisch Spectrum Twente, Enschede, The Netherlands) and processed within 6 h after drawing.

(ii) Labeling of target cells. To select leukocytes and leukocyte subpopulations, e.g., T lymphocytes, B lymphocytes, and $CD4^+$ cells, from whole blood, we labeled the target cells immunomagnetically using the following EasySep kits (StemCell Technologies, Canada): human CD45 (clone MEM28; isotype, mouse IgG1) depletion, CD3 (clone UCHT-1; isotype, mouse IgG1) positive selection, CD19 (clone AE-1; isotype, mouse IgG1) positive selection, and CD4 (clone QS4120; isotype, mouse IgG1) positive selection. Each kit comprises a specific antibody cocktail and a dispersion of EasySep magnetic nanoparticles and was used according to the manufacturer's specifications. AO (Molecular Probes) was used to stain nucleated cells.

By titration, the optimal volumes of antibody cocktail and magnetic-nanoparticle dispersion, concentration of AO, incubation time of reagents, and magnetic separation time were determined. The optimal amounts of antibody cocktail and nanoparticle dispersions for our experiments were found to be the following: 5 μl of CD45 cocktail and 10 μl of magnetic-nanoparticle dispersion, 10 μl of CD3 cocktail and 5 μl of magnetic-nanoparticle dispersion, 12 μl of CD19 cocktail and 6 μl of magnetic-nanoparticle dispersion, and 15 μl of CD4 antibody cocktail and 7.5 μl of nanoparticles.

(iii) Cell enumeration procedure. To 100 μl of whole blood, the appropriate volume of antibody cocktail was added and mixed. (For leukocyte enumeration, 100 μl of a 20-times-diluted blood sample was used). After a 15-min incubation, the corresponding volume of magnetic-nanoparticle dispersion was added and mixed. After another 10 min of incubation, AO (10 μl; 0.08 mM) was added, and the sample was diluted with system buffer (Immunicon Inc.) to a final volume of 410 μl. Approximately 340 μl of the diluted sample was then transferred to an analysis chamber. The chamber was plugged and placed in a magnet assembly (Magnest; Immunicon Inc.) as illustrated in Fig. 1B. After 20 min of magnetic separation, the analysis chamber was transferred into the Magnest inside the SP ICM instrument. Fluorescent images of the analysis surface were captured and analyzed. The measurement and image analysis took about 40 s.

(iv) Linearity. To evaluate the linearity of our system within the low-cell-count range (0 to 400/μl), a series of diluted blood samples containing graded, known numbers of CD3 T lymphocytes was prepared according to the following protocol. For a whole-blood specimen of a healthy donor, CD3 enumeration was performed by our system. Then the original whole-blood specimen was diluted with system buffer at different ratios, resulting in a series of six specimens with known numbers of CD3 T lymphocytes (12, 25, 50, 100, 200, and 400/μl). CD3 enumeration was performed for five replicates of each diluted blood sample. Linearity was evaluated.

SP and DP FCM methods. SP and DP FCM methods were both used to obtain absolute cell counts as controls in order to evaluate the accuracy of our SP ICM method and the interchangeability between our method and FCM.

For the SP FCM method, the TruCount method was used. The blood specimens were processed using a lyse–no-wash method according to the manufacturer's recommendations (BD Biosciences) and were analyzed with a FACSCalibur using CellQuest software (BD Biosciences) (20).

For the DP FCM method, the relative proportions of specific cell subpopulations were obtained with a FACSCalibur using CellQuest software. The absolute number of total leukocytes was determined by a Sysmex SE-9500 hematology analyzer (Sysmex Corporation, Japan).

For both FCM methods, the reagents used were fluorescein isothiocyanate (FITC)-conjugated CD3 [clone SK7; isotype, mouse IgG1(κ)], phycoerythrin (PE)-conjugated CD4 [clone SK3; isotype, mouse IgG1(κ)], peridinin chlorophyll protein (PerCP)-conjugated CD45 [clone 2D1; isotype, mouse IgG1(k)], FITC-conjugated CD3 [clone SK7; isotype, mouse IgG1(κ)], PE-conjugated CD19 [clone SJ25C1; isotype, mouse IgG1(κ)], and PerCP-conjugated CD45 [clone 2D1; isotype, mouse IgG1(κ)] (TriTEST; BD Biosciences), and FACS lysing solution (BD Biosciences).

Immunophenotyping of $CD4^+$ immunomagnetically selected cells. To determine the blood cell populations represented in immunomagnetically selected $CD4^+$ cells, we incubated the blood samples with CD4 immunomagnetic particles and immunofluorescent labels CD3 [clone UCHT-1; isotype, mouse IgG1(κ)]-allophycocyanin (APC), CD14 [clone MϕP9; isotype, mouse IgG2b(κ)]-PE, and CD66b [clone G10F5; isotype, mouse IgM(κ)]-FITC (BD Biosciences). AO was not added in this case. After sample incubation, the sample chamber/Magnest assembly was placed under a fluorescent microscope (ECLIPSE E400; Nikon, Japan) equipped with a 40× objective (numerical aperture, 0.6). Fluorescent images were taken from 10 randomly selected areas of the chamber surface using appropriate filters for FITC, PE, and APC. Blood specimens from three healthy donors were used.

Statistical analyses. To assess the test precision of the SP ICM method, we enumerated five replicates of fresh blood specimens from each of 27 patients. For each patient, the coefficient of variation (CV; calculated as standard deviation/mean × 100%) of the five cell counts was calculated, and the results were compared with the Poisson variation (see below).

To assess the accuracy of our method, we compared the SP ICM results with those of the SP and DP FCM methods. Based on the cell counts obtained from different methods, linear regression lines were drawn and correlation coefficients (R) were calculated. Bland-Altman plots (2, 3, 15, 17) were analyzed to determine the interchangeability between the methods. In the Bland-Altman plots, the average of the cell counts obtained by the two methods is plotted on the x axis, and the difference between the results by the two methods divided by the average, expressed as a percentage, is plotted on the y axis. The solid line in the plot represents the bias of the mean of the (difference/average) percentage between the two methods, and the dashed lines indicate the upper and lower limits of agreement (bias ± 1.96 standard deviations).

RESULTS

Design of ICM. Figure 1 shows the prototype of the ICM we built (Fig. 1A) and a scheme with the separate components of the ICM.

For magnetic separation, the incubated blood sample is transferred to an analysis chamber with inner dimensions of 30 mm (length) by 2.7 mm (width) by 4 mm (height). The chamber (outer) top surface is placed 2 mm below two magnetic poles of the Magnest. These poles, made of neodymium iron boron, have an internal magnetization of 13.7 kilogauss. The distance between the two poles is 3 mm, and the top angle of each pole piece is 20° (Fig. 1B). The force inside the chamber, generated by the magnetic gradient, points to the positive z direction of the chamber (also the axis of the objective) and has no components in the x or y axis. As a result, all immunomagnetically labeled cells move along the positive z direction to the upper surface of the chamber (Fig. 1B). Cells that have not been immunomagnetically labeled sediment to the bottom of the chamber due to gravity. The chamber/Magnest assembly is at 9° with respect to the horizontal plane, in order to move air bubbles out of the field of view. To eliminate the need for refocusing each time a new analysis chamber is placed into the magnet, spring-loaded ball bearings are applied, which push the upper surface of the chamber to a fixed position, ensuring a sharp image of the cells.

The layout of the optical design is shown in Fig. 1C. Two LEDs are placed symmetrically above the chamber, at an angle of 45° to the upper surface of the analysis chamber, to illuminate the region of interest. The maximum emission wavelength of the LEDs is 470 nm; this matches the absorption spectrum of AO. The fluorescence emitted by the AO-stained nucleated

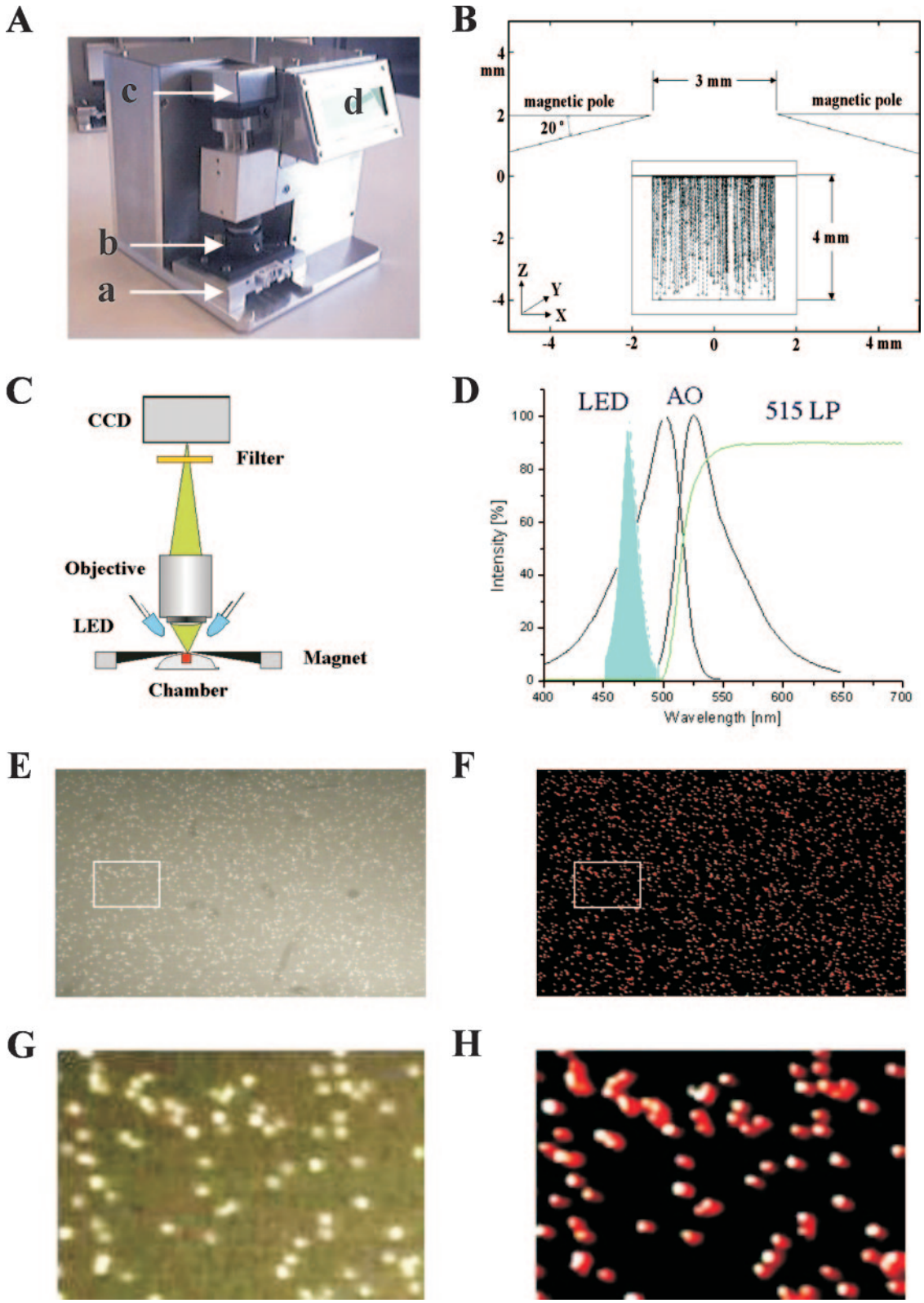

FIG. 1. (A) Prototype of the cell enumeration system. a, Magnest; b, objective; c, CCD camera; d, LCD. (B) Schematic representation of the trajectory of magnetically labeled objects. Dashed lines inside the chamber illustrate the trajectories of the cells that move up due to the magnetic force, starting from different positions. (C) Schematic representation of the optical design. (D) Spectra of the LED (emission), AO (excitation and emission), and the 515-nm long-pass filter (LP). (E) Recorded image of cells stained with AO. (F) Processed image from panel E. Red dots represent the events that have been counted as cells. (G and H) Enlarged images from the selected areas shown in panels E and F, respectively.

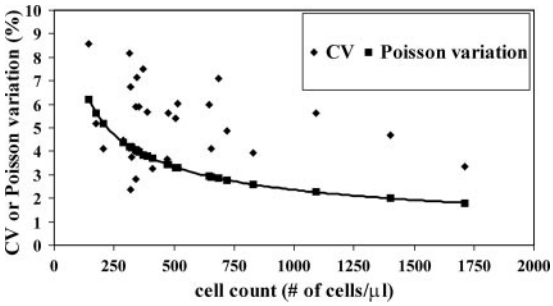

FIG. 2. CVs and Poisson variations of leukocyte counts from five replicates of each of the blood samples (20 times diluted) of 27 patients plotted against their mean leukocyte counts.

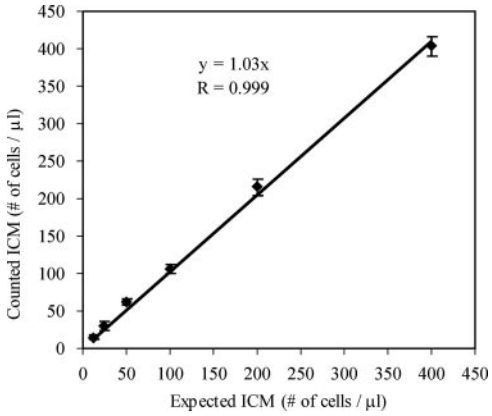

FIG. 3. Linearity of our system in the low-cell-count range (0 to 400 CD3 T lymphocytes/μl). Error bar, standard deviation of five replicates of CD3 T lymphocyte counts.

cells is collected by a 10× objective (numerical aperture, 0.2), which is perpendicular to the analysis surface; then the fluorescence is filtered through a 515-nm long-pass filter. The image is focused on the CCD surface of a smart camera. The camera is programmable in C++ and can be used to analyze the images. The spectra of the LED, AO, and the long-pass filter are shown in Fig. 1D.

To start a cell counting cycle, the analysis chamber is inserted into the instrument. A microswitch triggers the measurement cycle. The LEDs illuminate the sample for 2 s, and a fluorescence image is captured. Then the image is processed by the image analysis algorithm. The total time required to capture and analyze an image, and to display the cell count per microliter of whole blood on the LCD, is approximately 40 s.

Typical images before and after analysis are shown in Fig. 1E and F, respectively. Figure 1G and H show the enlarged images from the selected areas in Fig. 1E and F, respectively. Each figure represents an analyzed image area of 1.85 mm^2 (1.53 mm by 1.21 mm). Since the height of the chamber (inside distance) is 4 mm and the blood sample has been diluted 4.1-fold (or 82-fold for leukocyte enumeration), the cells shown in each image correspond to those originally present in 1.80 μl of whole blood (or a 20-times-diluted blood sample for leukocyte enumeration).

Evaluation of SP ICM. (i) Precision. To assess the test precision of our system, leukocytes of five replicates from each of the blood samples of 27 patients were enumerated (135 measurements in total). From cell counts of the replicates of each blood sample, the CV (standard deviation/mean × 100%) was determined. Assuming that the distribution of the cell counts of the five replicate samples follows a Poisson distribution, the expected statistical Poisson variation of the cell count can be estimated as $[\sqrt{1.8\ \mu l \times (\text{cell count}/\mu l)}]/[1.8\ \mu l \times (\text{cell count}/\mu l)] \times 100$, where the cell count/μl is based on the total sampling of 1.8 μl of the 20-times-diluted blood samples.

Figure 2 shows the Poisson variations and CVs of each of the 27 blood samples versus their mean leukocyte counts. The mean leukocyte counts of these blood samples (20 times diluted) ranged from 145/μl to 1,712/μl; correspondingly, the Poisson variations range from 6.19% to 1.80%. The measured CVs ranged from 2.38% to 8.56% for these 27 blood samples. In most cases, the measured CV is slightly higher than the Poisson variation, indicating that the precision of our system is mostly determined by Poisson statistics, although other errors, e.g., sampling errors, are present.

(ii) Linearity. To evaluate the linearity of our system, CD3 enumeration was performed on a whole-blood sample, and a series of diluted blood samples containing graded, known numbers of CD3 T lymphocytes (12, 25, 50, 100, 200, and 400/μl) was prepared. In Fig. 3, the measured CD3 T-lymphocyte counts are plotted as a function of the expected CD3 T-lymphocyte counts of these samples. The error bar represents the standard deviation for five replicates of CD3 T-lymphocyte counts. A linear relation (slope, 1.03; $R = 0.999$) was found, demonstrating the linearity of our system in the low-cell-count range (0 to 400/μl).

(iii) Accuracy of SP ICM in counting cells with specific antibodies. To determine the accuracy of our method, leukocytes (blood specimens of 50 patients), T lymphocytes (blood specimens of 52 patients), and B lymphocytes (blood specimens of 42 patients) were enumerated by our method and by the SP and DP FCM methods. For enumeration of these cells by SP ICM, immunomagnetic selection is governed by antibody specificity, i.e., these cells are uniquely labeled using the specific antibodies. Table 1 summarizes the correlation coefficients (R) and the slopes of the linear regression lines, and Table 2 presents the biases obtained from the Bland-Altman plots.

First, the results obtained by our SP ICM method and those obtained by the TruCount method were compared. Figure 4A to C show for the different cell populations the linear regression lines comparing the cell counts obtained by these two methods. The correlation coefficients (R) and slopes are also given. In parallel, Bland-Altman plots are given in Fig. 5A to C. The bias between the two methods and the upper and lower limits of agreement are indicated.

For leukocytes and T lymphocytes, our enumeration method shows a good correlation with TruCount (R, 0.95 and 0.97, respectively). However, the slopes of the linear regression lines for these populations (0.89 for leukocytes and 0.86 for T lymphocytes) show that the results obtained by our method for those populations are about 11% to 14% lower than those by TruCount. In agreement with this observation, the Bland-Alt-

TABLE 1. Correlations among cell counts obtained by our cell enumeration system (SP ICM), TruCount, and DP data for different cell populations

Comparison	Linear regression for the following cell type (antibody)[a]:							
	Leukocytes (CD45)		T lymphocytes (CD3)		B lymphocytes (CD19)		T lymphocytes (CD4)	
	R	Slope	*R*	Slope	*R*	Slope	*R*	Slope
ICM vs TruCount	0.95	0.89	0.97	0.86	0.96	1.01	0.83	1.42
ICM vs DP	0.97	1.14	0.97	1.09	0.95	1.23	0.85	1.75
TruCount vs DP	0.98	1.26	0.98	1.26	0.99	1.23	0.97	1.24

[a] The number of patients was 50 for leukocytes (CD45), 52 for $CD3^+$ T lymphocytes, 42 for B lymphocytes (CD19), and 45 for $CD4^+$ T lymphocytes.

man plots show a bias of approximately 10% (TruCount versus SP ICM).

For B lymphocytes, the results are different: the correlation coefficient between SP ICM and TruCount (*R*) is 0.96, whereas both the slope of the linear regression line (1.01) and the bias of the Bland-Altman plot (0.3% [TruCount versus SP ICM]) indicate excellent agreement between the SP ICM and the TruCount method for enumerating B lymphocytes.

Similar analyses were performed for comparison of the results obtained by our SP ICM method with those by the DP FCM method (see Tables 1 and 2). The SP ICM shows a good correlation with DP FCM for enumerating leukocytes (the DP FCM leukocyte count was directly obtained by a hematology analyzer) ($R = 0.97$) and T lymphocytes ($R = 0.97$). However, the slopes of the linear regression lines for these populations (1.14 and 1.09, respectively) show that cell counts by our method are about 9 to 14% higher than those by the DP FCM method. Bland-Altman plots for the same populations show a bias of −12.0 to −12.9% (DP FCM versus SP ICM).

Again, the results for B lymphocytes are different: the correlation coefficient is good ($R = 0.95$), but both the slope of the regression line (1.23) and the bias of the Bland-Altman plot (−20.1% [DP FCM versus SP ICM]) indicate that the B-lymphocyte count obtained by DP FCM is about 20% lower than that by our SP ICM method.

We also performed the same comparison between the TruCount and DP FCM methods. For enumeration of leukocytes, T lymphocytes, and B lymphocytes, good correlations between TruCount and DP FCM were obtained (*R*, 0.98 to 0.99). The TruCount data are about 25% higher than those obtained from DP FCM (slope, 1.23 to 1.26; bias, 20.5% to 22.8% [TruCount versus DP FCM]).

It should be noted that in Fig. 4B, when the T-lymphocyte cell counts obtained by the TruCount method are in excess of 2,000/μl, most of the dots (SP ICM cell counts plotted against TruCount data) are located lower than the linear regression line. In parallel, in the corresponding Bland-Altman plot (Fig. 5B), when the TruCount data are higher than 2,000/μl, all the plotted dots locate in regions above the bias line (TruCount versus SP ICM). These results are related to the limitation of the image analysis algorithm in our system: when the cell counts are above 2,000/μl, i.e., the number of cell events is more than ca. 3,600 per image (1 image corresponds to 1.8 μl of blood sample), some of the cells are too close to each other and therefore cannot be counted separately; this results in underestimation of the cell counts.

(iv) $CD4^+$ cell enumeration. In contrast to leukocytes and leukocyte subpopulations that are uniquely defined by one specific type of cell surface antigen, as described above, $CD4^+$ cells comprise $CD4^+$ T lymphocytes and $CD4^{dim}$ monocytes. Because the $CD4^+$ T-lymphocyte count is essential for HIV staging, the applicability of our SP ICM system to the counting of $CD4^+$ cells is evaluated.

For $CD4^+$ cell enumeration, the correlation coefficients for SP ICM data with TruCount ($R = 0.83$ [Fig. 4D]) and DP ($R = 0.85$) data were significantly lower than those for leukocytes and leukocyte subpopulations. SP ICM $CD4^+$ cell counts are higher than $CD4^+$ T-lymphocyte counts obtained by TruCount and by the DP FCM method: the slopes of the linear regression lines are 1.42 and 1.75, respectively, and the biases are −37.5% (TruCount versus SP ICM [Fig. 5D]) and −56.4% (DP FCM versus SP ICM), respectively.

Immunophenotyping of $CD4^+$ immunomagnetically selected cells. To identify the cell types other than $CD4^+$ T lymphocytes that are counted as $CD4^+$ cells by SP ICM, immunophenotyping of immunomagnetically selected $CD4^+$ cells was performed. In this experiment, CD4 immunomagnetically selected cells were stained with CD3-APC, CD14-PE, and CD66b-FITC. Figure 6 shows the corresponding images ob-

TABLE 2. Biases among cell counts obtained by our cell enumeration system (SP ICM), TruCount, and DP data for different cell populations

Comparison[a]	Bias from Bland-Altman plot (%) for the following cell type (antibody)[b]:			
	Leukocytes (CD45)	T lymphocytes (CD3)	B lymphocytes (CD19)	T lymphocytes (CD4)
(TruC − ICM)/avg (%) vs avg	10.1	10.0	0.3	−37.5
(DP − ICM)/avg (%) vs avg	−12.0	−12.9	−20.1	−56.4
(TruC − DP)/avg (%) vs avg	22.0	22.8	20.5	20.0

[a] Expressed as the difference between the results by two methods divided by the average of those results, expressed as a percentage, versus the average of the results obtained by the two methods. TruC, TruCount.

[b] The number of patients was 50 for leukocytes (CD45), 52 for $CD3^+$ T lymphocytes, 42 for B lymphocytes (CD19), and 45 for $CD4^+$ T lymphocytes.

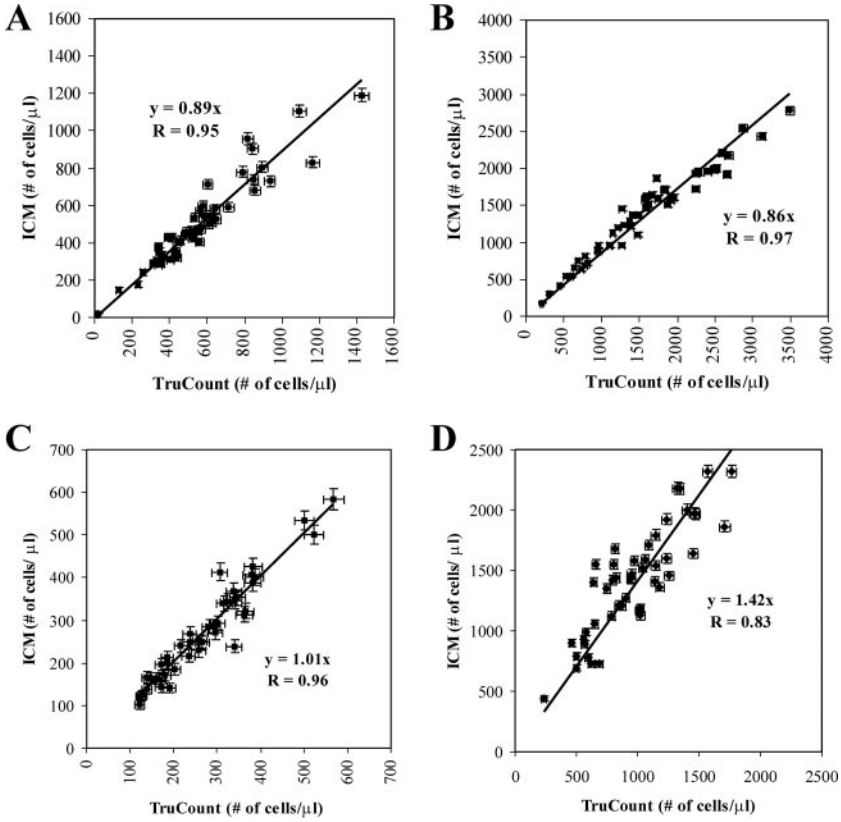

FIG. 4. Linear regressions of cell counts by our cell enumeration system (SP ICM) and TruCount for leukocytes (20-times-diluted whole blood) (A), T lymphocytes (B), B lymphocytes (C), and $CD4^+$ T lymphocytes (D). Blood specimens for 42 to 52 patients were analyzed (for details, see Table 1). The error bar for each dot represents the square root of the value.

tained using appropriate filters in which different types of cells on the same area of the chamber upper surface are depicted.

Thirty T lymphocytes stained with CD3-APC, one monocyte stained with CD14-PE, and two granulocytes stained with CD66b-FITC, as shown in Fig. 6A to C, respectively. As we can see from these images, monocytes and granulocytes can also be selected by CD4 immunomagnetic labeling. To get an idea of the composition of the total CD4 cell counts, blood specimens of three healthy donors were tested by immunophenotyping. The average counts of $CD4^+$ T lymphocytes, monocytes, and granulocytes were 808, 422, and 70 cells/μl, respectively. In these experiments the total CD4 count contained 32.5% monocytes (27.0%, 42.1% and 28.4% for each donor, respectively) and 5.4% granulocytes (5.1%, 6.0% and 5.2%, respectively).

DISCUSSION

The results demonstrate that the precision and the linearity of our immunomagnetic SP ICM system are excellent.

In our study, the cell counts of leukocytes and leukocyte subpopulations (T and B lymphocytes) obtained from SP FCM (TruCount) and DP FCM (DP data) technologies showed excellent correlations (*R*, 0.97 to 0.99). The TruCount counts of leukocytes and leukocyte subpopulations were approximately 21% higher than the corresponding DP counts (biases, 20.5% to 22.8%) (Tables 1 and 2). Since DP data were obtained by multiplying the relative proportions of lymphocyte subpopulations obtained by FCM by the absolute number of total leukocytes obtained from the hematology analyzer, the difference in cell counts of leukocyte subpopulations can be ascribed to the fact that the leukocyte count by TruCount is 22% higher than that by the hematology analyzer in DP FCM.

This 22% difference in leukocyte counts from TruCount and from the hematology analyzer can be explained by two possible reasons. First, we found that about 10% of the calibration beads applied in the TruCount method are aggregates of two or even three. This may induce a 10% or even higher overcount in TruCount. Such an overcount in SP cytometric methods using calibration beads has been reported (5). Second, such a difference between two methods or between two laboratories is normal (16). For example, a collaborative study of 280 laboratories for CD4 enumeration showed a mean interlaboratory CV of 13.7% (range, 10 to 18.3%) for the SP method and 23.4% (range, 14.5 to 43.7%) for the DP method (1). Consequently, the difference we observed between TruCount and the DP data is acceptable.

Our cell enumeration method shows good correlations and agreements with the TruCount and DP methods for counting well-defined cell populations that have a unique cell membrane antigen: For CD45 leukocytes and CD3 T lymphocytes, the cell counts by our method are in between the TruCount and the DP data, and the biases between our method and the two FCM methods are less than ±13%. Since these biases can

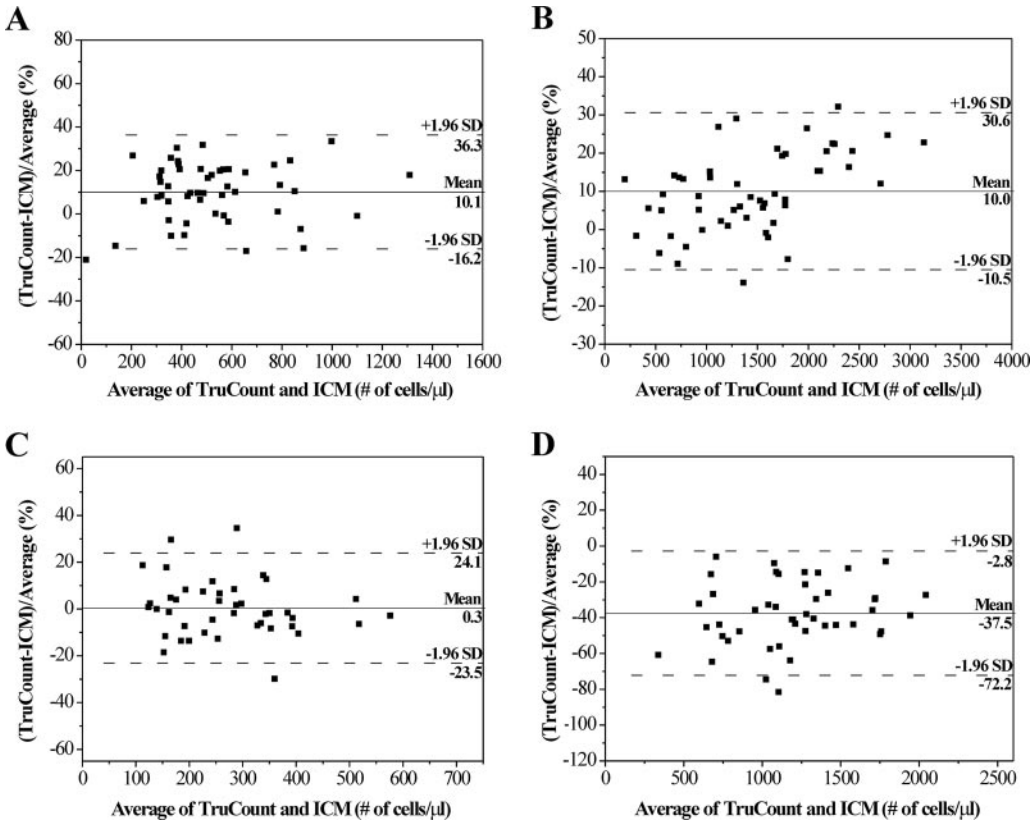

FIG. 5. Bland-Altman plots comparing cell counts generated by our cell enumeration system (SP ICM) and TruCount for leukocytes (20-times-diluted whole blood) (A), T lymphocytes (B), B lymphocytes (C), and $CD4^+$ T lymphocytes (D).

be explained by the same reasons we discussed above, it is demonstrated that our SP ICM system is comparable to both FCM technologies. For CD19 B lymphocytes, cell counts obtained by our method showed no significant difference from the TruCount data (bias, 0.3%) but were 20.1% higher than the DP data. This discrepancy may be related to the fact that different leukocyte subpopulations have different sensitivities to the red blood cell lysing buffers used in the immunophenotyping processes in FCM methods. (These red blood cell lysing buffers may induce membrane destruction and could result in significantly lower leukocyte counts. This effect is leukocyte subpopulation dependent and even individual dependent due to the patient disease and the drug treatment [9, 10]). It may also be related to the different isotypes of CD19 antibodies used in these two methods.

It can therefore be concluded that our method is verified for counting leukocytes and T and B lymphocytes.

For CD4 cell enumeration, as can be expected and as was proven by immunophenotyping, our method counts both $CD4^+$ T lymphocytes and $CD4^{dim}$ monocytes. When an anti-

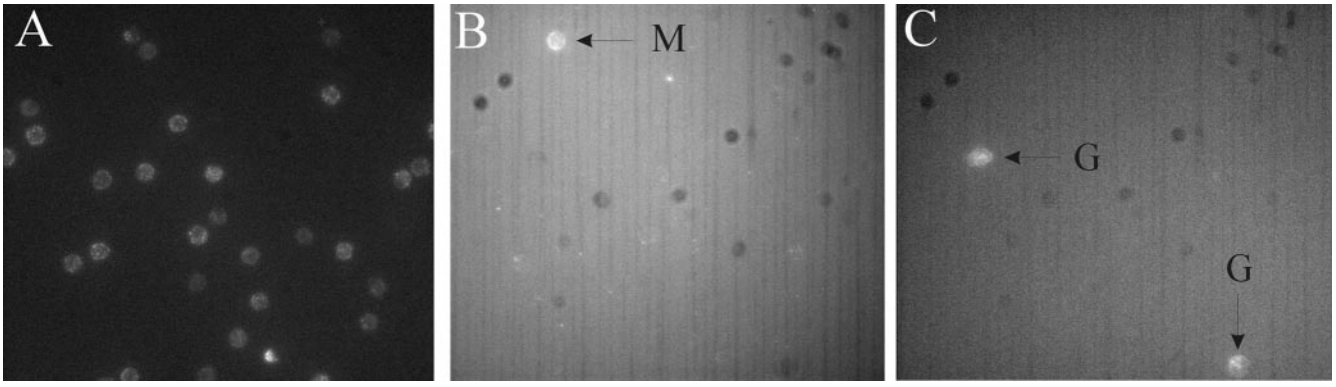

FIG. 6. Immunophenotyping of cells immunomagnetically selected with CD4. (A) Thirty CD3-APC-stained $CD4^+$ T lymphocytes; (B) one CD14-PE-stained monocyte (M); (C) two CD66b-FITC-stained granulocytes (G). All panels show fluorescence images from the same area on the upper surface of the chamber. The dark particles in panels B and C are red blood cells that adhered to the upper surface of the chamber.

CD4 antibody is used to immunoselect $CD4^+$ cells, some of the monocytes, which have bound enough magnetic nanoparticles to overcome the gravity and viscosity of the sample solution in the magnetic field, could be collected at the upper surface of the chamber and counted as $CD4^+$ cells. In addition, a small amount of granulocytes, which represent the largest leukocyte subpopulation, could nonspecifically bind immunomagnetic nanoparticles and be attracted to the upper surface of the chamber during the magnetic selection of the $CD4^+$ cells.

It should be noted that for CD3 T-lymphocyte and CD19 B-lymphocyte enumeration, the nonspecific binding of granulocytes was prevented, since the CD3 and CD19 cocktails employed contain an antibody against human Fc receptor and prevent the nonspecific binding of the magnetic nanoparticles to granulocytes (from the product data sheet). Unfortunately, this antibody is absent in the CD4 cocktail we used.

We conclude that with our immunomagnetic SP ICM system, antibody-specific cell enumeration can be successfully applied with CD45, CD3, and CD19. The immunomagnetically selected $CD4^+$ cells contain both $CD4^+$ T lymphocytes and $CD4^{dim}$ monocytes. This clearly shows the well-known problem of monocyte interference with CD4 counts in HIV staging (11, 12). Nevertheless, immunophenotyping results suggest that the $CD4^+$ T lymphocytes could be enumerated in our immunomagnetic SP ICM system by applying additional CD3 immunofluorescent labeling. New immunomagnetic volumetric systems, which use extra immunofluorescence labeling to achieve absolute $CD3^+$ $CD4^+$ T-lymphocyte counts, have been developed, and the results for $CD4^+$ T-lymphocyte enumeration will be presented in our forthcoming paper. These systems could then play a role in HIV staging in resource-constrained countries.

A major advantage of our cell enumeration system is that it is simple and easy to handle for sample preparation and measurement, even for less trained operators. No data interpretation is needed, which prevents subjective errors. The instrument is portable, operates on a rechargeable battery, has no moving parts, and needs no fluidics. Its simplicity allows the development of affordable systems suitable for various applications. The single-unit component price of the instrument is about US$4,400, much less than the cost of a flow cytometer (US$20,000 to $80,000) (14). Currently, the assay price is about US$7.5 for CD45 and CD3 enumeration and about US$10.0 for CD19 enumeration. The EasySep reagents are expensive and account for most of the cost. It would be ideal to apply cheaper immunonanoparticle reagents. Replacing the disposable chamber (ca. US$2.3) with a cheaper one may further decrease the cost per test. Another potential advantage of this method is that the blood samples can be prepared and held in the chamber/magnet assembly for at least 10 h at room temperature in the dark, which could be useful in field situations. These features may permit the usage of the instrument under harsh environmental conditions in resource-constrained countries. Moreover, we have demonstrated that it is reliable by comparisons with the TruCount and DP FCM technologies.

ACKNOWLEDGMENTS

We thank I. Vermes and C. H. H. ten Napel from MST hospital in Enschede, The Netherlands, for kindly supplying fresh blood specimens and hematology data. We acknowledge all patients and healthy donors whose blood specimens were tested in this study.

Part of the project is financially supported by STW, the Dutch Technology Foundation (project TGT.6146).

REFERENCES

1. **Barnett, D., V. Granger, L. Whitby, I. Storie, and J. T. Reilly.** 1999. Absolute $CD4^+$ T-lymphocyte and $CD34^+$ stem cell counts by single-platform flow cytometry: the way forward. Br. J. Haematol. **106:**1059–1062.
2. **Bland, J. M., and D. G. Altman.** 1986. Statistical methods for assessing agreement between two methods of clinical measurement. Lancet **i:**307–310.
3. **Boyle-Whitesel, M. J., H. J. Norton, and W. Anderson.** 1997. A critical assessment of the techniques used to determine agreement between two methods of clinical measurement, p. 309. *In* Proceedings of the American Statistical Association Section on Statistical Education. American Statistical Association, Alexandria, VA.
4. **Brand, A., L. M. van de Watering, and F. H. Claas.** 2000. Clinical significance of leukoreduction of blood components. Vox Sang. **78**(Suppl. 2)**:**227–229.
5. **Brando, B., W. Göhde, Jr., B. Scarpati, and G. D'Avanzo.** 2001. The "vanishing counting bead" phenomenon: effect on absolute $CD34^+$ cell counting in phosphate-buffered saline-diluted leukapheresis samples. Cytometry **43:** 154–160.
6. **Centers for Disease Control and Prevention.** 1997. Revised guidelines for performing $CD4^+$ T-cell determinations in persons infected with human immunodeficiency virus (HIV). Morb. Mortal. Wkly. Rep. **46:**1–29.
7. **Denny, T. N., D. Stein, T. Mui, A. Scolpino, and B. Holland.** 1996. Quantitative determination of surface antibody binding capacities of immune subsets present in peripheral blood of healthy adult donors. Cytometry **26:**265–274.
8. **Dietz, L. J., R. S. Dubrow, B. S. Manian, and N. L. Sizto.** 1996. Volumetric capillary cytometry: a new method for absolute cell enumeration. Cytometry **23:**177–186.
9. **Göhde, W., U. Cassens, L. G. Lehman, Y. Traorè, W. Göhde, Jr., P. Berkes, C. Westerberg, and B. Greve.** 2003. Individual patient-dependent influence of erythrocyte lysing procedures on flow-cytometric analysis of leukocyte subpopulations. Transfus. Med. Hemother. **30:**165–170.
10. **Greve, B., C. Beller, U. Cassens, W. Sibrowski, E. Severin, and W. Göhde.** 2003. High-grade loss of leukocytes and hematopoietic progenitor cells caused by erythrocyte-lysing procedures for flow cytometric analyses. J. Hematother. Stem Cell Res. **12:**321–330.
11. **Janossy, G.** 2004. Dried blood spot technology for $CD4^+$ T-cell counting. Lancet **363:**1074.
12. **Janossy, G.** 2004. Clinical flow cytometry, a hypothesis-driven discipline of modern cytomics. Cytometry A **58:**87–97.
13. **Larson, C. J., J. G. Moreno, K. J. Pienta, S. Gross, M. Repollet, S. M. O'hara, T. Russell, and L. W. M. M. Terstappen.** 2004. Apoptosis of circulating tumor cells in prostate cancer patients. Cytometry A **62:**46–53.
14. **Medical Mission Institute.** 2001. Access to antiretroviral therapy in developing countries: a continuum of care approach. Guidelines and policy issues: appropriate laboratory methods in the management of HIV infection. CI/CIDSE Policy Workshop. Medical Mission Institute, Wuerzburg, Germany.
15. **Meijer, P.** 2003. Method comparison: correlation is not enough to decide about agreement and clinical accuracy. Thromb. Haemost. **90:**555–556.
16. **Nicholson, J. K. A., D. Stein, T. Mui, R. Mack, M. Hubbard, and T. Denny.** 1997. Evaluation of a method for counting absolute numbers of cells with a flow cytometer. Clin. Diagn. Lab. Immunol. **4:**309–313.
17. **Pollock, M. A., S. G. Jefferson, J. W. Kane, K. Lomax, G. MacKinnon, and C. B. Winnard.** 1992. Method comparison—a different approach. Ann. Clin. Biochem. **29:**556–560.
18. **Racila, E., D. Euhus, A. J. Weiss, C. Rao, J. McConnell, L. W. M. M. Terstappen, and J. W. Uhr.** 1998. Detection and characterization of carcinoma cells in the blood. Proc. Natl. Acad. Sci. USA **95:**4589–4594.
19. **Robinson, G., L. Morgan, M. Evans, S. McDermott, S. Pereira, M. Wansbrough-Jones, and G. Griffin.** 1992. Effect of type of haematology analyser on CD4 count. Lancet **340:**485.
20. **Schnizlein-Bick, C. T., J. Spritzler, C. L. Wilkening, J. K. A. Nicholson, M. R. G. O'Gorman, site investigators, and the NIAID DAIDS New Technologies Evaluation Group.** 2000. Evaluation of TruCount absolute-count tubes for determining CD4 and CD8 cell numbers in human immunodeficiency virus-positive adults. Clin. Diagn. Lab. Immunol. **7:**336–343.
21. **Shapiro, H. M.** 2004. Cellular astronomy. Cytometry A **60:**115–124.
22. **Tibbe, A. G. J., B. G. de Grooth, J. Greve, G. J. Dolan, C. Rao, and L. W. M. M. Terstappen.** 2002. Magnetic field design for selecting and aligning immunomagnetic labeled cells. Cytometry **47:**163–172.